# Optical bistability and tristability in nonlinear metal/dielectric composite media of nonspherical particles

Lei Gao,[1,2,*] Liping Gu,[2,3] and Zhenya Li[1,2]
[1]*CCAST (World Laboratory), P.O. Box 8730, Beijing 100080, China*
[2]*Department of Physics, Suzhou University, Suzhou 215006, China*
[3]*Department of Physics, Changshu Institute of Technology, Changshu 215500, China*
(Received 8 April 2003; revised manuscript received 6 August 2003; published 3 December 2003)

Based on a spectral representation method and a self-consistent mean field theory, we present a general framework to investigate the optical bistability in a nonlinear two-phase composite, where spheroidal metallic inclusions are randomly oriented and embedded in a dielectric host. The relation between the spatial average of the local field squared $\langle|E|^2\rangle_i$ $(i=1,2)$ and the external field squared $E_0^2$ is obtainable through the spectral density function which is predicted from our recently derived Maxwell-Garnett approximation. In addition to single optical bistability (OB), the appearance of double OB and optical tristability (OT) is reported, and the corresponding phase diagram is given. We find that the regions of the single OB, the double OB, and the OT are dependent on the shape and volume fraction of the metallic particles. Our method allows us to take one step forward to study some field-dependent effective optical properties, such as the refractive index, extinction coefficient as well as reflectance. The general framework is also applied to investigate exactly the solvable composites consisting of nonlinear spheroidal inclusions and linear dielectric host in the dilute limit. To this end, the present method is shown to be in excellent agreement with the exact solution. In addition, the present method predicts a larger threshold intensity than the variational approach.

DOI: 10.1103/PhysRevE.68.066601 PACS number(s): 42.65.Pc, 42.65.An, 81.05.Rm, 78.20.−e

## I. INTRODUCTION

Because of its potential applications for optical logic, optical memory element, and optical switching devices, the phenomenon of intrinsic optical bistability in composite media has received much attention [1–4]. To obtain the optical bistable behavior, the composite materials are usually made of a dielectric host and metallic (or semiconductor) granular inclusions, whose dielectric constant contains a negative real part and a small imaginary part. Moreover, the component(s) must possess nonlinear dielectric responses. Proposals have been put forward to decrease the intensity threshold for the bistability by exploiting the field enhancement produced by the surface plasmon resonance of the composite media [2–4].

In general, the problem of calculating the effective nonlinear properties in nonlinear composite materials is quite intractable. Thus, the investigations on optical bistable behavior were mainly limited to some exactly solvable microstructures such as those low density mixtures, parallel slabs, and so on. In previous works [5,6], a variational approach was developed to investigate the bistable behavior in a weakly nonlinear composite medium. When the applied intensity $|E_0|^2$ is strong, the dielectric constant of the nonlinear component will strongly be relevant to the local field within it. Therefore, the weak field nonlinearity is not valid any more.

In experiment, Neuendorf *et al.* [7] reported the observation of the bistability of nanometer-sized spherical CdS particles coated with silver. Motivated by this observation, Yuen and Yu [8] studied the nonlinear composites of coated spheres, and obtained the optimal conditions for the bistable operation by adjusting the thickness of coatings. On the other hand, it was shown that the threshold intensity for the optical bistability can also be optimized by the suitable adjustment of the particle shape of ellipsoidal inclusions [4,9,10]. However, as we know, the ellipsoidal inclusions were assumed to be randomly distributed but oriented with respect to one another, and the theoretical results were only valid for a particular orientation of the particles.

For realistic composites, the individual granular inclusion is not perfectly aligned and even randomly oriented. We have shown that the effective optical nonlinearity of the weakly nonlinear composite system of ellipsoidal particles oriented in the same direction [11] is quite different from that of randomly oriented ellipsoidal particles [12]. In this paper, based on a self-consistent mean field approximation [13–15] in combination with a spectral representation method [16], we will put forth a general framework, in an attempt to investigate the optical bistable behavior of nonlinear metal/dielectric composite media, in which randomly oriented spheroidal particles are distributed in the dielectric host in the presence of a strong external applied electric field. In detail, we will perform numerical calculations with a focus on the relation between the average of the local field squared inside the metallic inclusions $\langle|E|^2\rangle_1$ (instead of $\langle|E|\rangle_1$ [17]) and the external field intensity $E_0^2$. To our interest, the appearance of double bistability and tristability in contrast to single bistability will be shown, and the phase diagram between them is given. Moreover, our method provides an easy way to study the effective nonlinear optical properties as a function of the external field, such as the refractive index, extinction coefficient, and reflectance. For increasing $E_0$,

*Email address: lgaophys@pub.sz.jsinfo.net

 

such physical parameters can exhibit quite complex behaviors.

## II. THEORY

### A. Spectral representation theory and self-consistent mean field approximation

Let us first consider a linear two-constituent composite consisting of one component of dielectric constant $\epsilon_1$ and volume fraction $f$, and the other component of $\epsilon_2$ and $1-f$.

In the presence of a uniform external applied electric field $\mathbf{E}_0 \equiv E_0 \mathbf{e}_z$, with $\mathbf{e}_z$ being the vector along the $z$ axis, the electrostatic potential in the quasistatic limit obeys the Laplace equation:

$$\nabla \cdot \left[ \left( 1 - \frac{1}{s} \eta(\mathbf{r}) \right) \nabla \phi(\mathbf{r}) \right] = 0, \tag{1}$$

with appropriate boundary conditions, where $s \equiv \epsilon_2/(\epsilon_2 - \epsilon_1)$ is the material parameter and $\eta(\mathbf{r})$ is the characteristic step function (which is equal to unity in component 1 and zero in component 2). The electric potential $\phi(\mathbf{r})$ can be solved formally

$$\phi(\mathbf{r}) = -E_0 z + \frac{1}{s} \int d\mathbf{r}' \, \eta(\mathbf{r}') \nabla' G(\mathbf{r} - \mathbf{r}') \cdot \nabla \phi(\mathbf{r}'), \tag{2}$$

where $G(\mathbf{r}-\mathbf{r}') \equiv 1/(4\pi|\mathbf{r}'-\mathbf{r}|)$ is the free-space Green's function.

In order to obtain the solution of Eq. (1), we introduce an integral-differential Hermitian operator $\hat{\Gamma}$, which satisfies

$$\hat{\Gamma} \phi(\mathbf{r}) \equiv \int d\mathbf{r}' \, \eta(\mathbf{r}') \nabla' G(\mathbf{r}' - \mathbf{r}) \cdot \nabla' \phi(\mathbf{r}'), \tag{3}$$

and the corresponding inner product

$$\langle \phi | \psi \rangle = \int d\mathbf{r} \, \eta(\mathbf{r}) \nabla \phi^* \cdot \nabla \psi. \tag{4}$$

Then Eq. (2) can be simplified to

$$\phi(\mathbf{r}) = -E_0 z + \frac{1}{s} \hat{\Gamma} \phi(\mathbf{r}). \tag{5}$$

Let $s_n$ and $\phi_n(\mathbf{r})$ be the $n$th eigenfunction and eigenvalue of the $\hat{\Gamma}$ operator. The potential $\phi(\mathbf{r})$ can be expanded in a series of eigenfunctions,

$$\phi(\mathbf{r}) = -\sum_n \frac{s \langle n|z \rangle}{s - s_n} \phi_n(\mathbf{r}) E_0 \quad \text{in component 1} \tag{6}$$

and

$$\phi(\mathbf{r}) = -E_0 z - \sum_n \frac{s_n \langle n|z \rangle}{s - s_n} \phi_n(\mathbf{r}) E_0 \quad \text{in component 2.} \tag{7}$$

Within the Bergman-Milton spectral representation [16], the effective dielectric constant $\epsilon_e$ can be written as

$$\begin{aligned} \epsilon_e = \frac{\langle D_z \rangle}{E_0} &= \frac{-1}{E_0 V} \int d\mathbf{r} \epsilon_2 \left[ 1 - \frac{1}{s} \eta(\mathbf{r}) \right] (\mathbf{e}_z \cdot \nabla \phi) \\ &= \epsilon_2 \left[ 1 - \sum_n \frac{f_n}{s - s_n} \right], \end{aligned} \tag{8}$$

where $\langle \cdots \rangle$ denotes the spatial average, while the poles $s_n$ and residues $f_n \equiv |\langle n|z \rangle|^2$ are all confined to the real regions $0 \leqslant s_n, f_n \leqslant 1$ with $\Sigma_n f_n = 1$.

When the operator $\hat{\Gamma}$ has a continuous spectrum, Eq. (8) should be replaced with an integral form

$$\epsilon_e = \epsilon_2 \left[ 1 - \int \frac{m(x)}{s - x} dx \right], \tag{9}$$

where the spectral density function $m(x)$ is obtained through a limiting process,

$$m(x) = \lim_{\xi \to 0^+} \frac{1}{\pi} \mathrm{Im} \left[ \frac{\epsilon_e}{\epsilon_2} (s = x + i\xi) \right]. \tag{10}$$

Within the spectral representation, the spatial average of the local field squared in component 1 is found to be [16,18]

$$\begin{aligned} f \langle |E^2| \rangle_1 &= \frac{1}{V} \int_1 d\mathbf{r} |E|^2 = \frac{1}{V} \int_1 d\mathbf{r} \nabla \phi^* \cdot \nabla \phi \\ &= \frac{1}{V} \sum_n \sum_m \frac{|s|^2 \langle z|n \rangle \langle m|z \rangle}{(s^* - s_n)(s - s_m)} \int_1 d\mathbf{r} \nabla \phi_n^* \cdot \nabla \phi_m E_0^2 \\ &= \sum_n \frac{|s|^2 f_n}{|s - s_n|^2} E_0^2. \end{aligned} \tag{11}$$

Again, for a continuous spectrum, we have

$$f \langle |E|^2 \rangle_1 = \int_0^1 \frac{|s|^2 m(x)}{|s - x|^2} dx E_0^2. \tag{12}$$

Similarly, the spatial average of the local field squared inside component 2 can be expressed as [18]

$$(1-f) \langle |E|^2 \rangle_2 = \left[ 1 - \int_0^1 \frac{(|s|^2 - x) m(x)}{|s - x|^2} dx \right] E_0^2. \tag{13}$$

Equations (12) and (13) are derived under the assumption that both components are linear. In the present paper, they will be generalized to treat the composites where the two components are both nonlinear, and have the local constitutive relation between the electric displacement $\mathbf{D}$ and the field $\mathbf{E}$ as

$$\mathbf{D} = \epsilon_i \mathbf{E} + \chi_i |E|^2 \mathbf{E} = (\epsilon_i + \chi_i |E|^2) \mathbf{E}. \tag{14}$$

It is worth remarking that, in previous works [5,11,12,18], the relation between $\mathbf{D}$ and $\mathbf{E}$ is weakly nonlinear, i.e., the

contribution of the second (nonlinear) part in the right-hand side of Eq. (14) is less than that of the first (linear) part. As an extension, this limit is no longer necessary in the present paper.

To observe the optical bistable behavior, we must solve for the local field in both components. Because of the difficulty in finding the local field exactly, we resort to the mean field approximation, which amounts to approximating the nonlinear component with dielectric property [13–15]:

$$\tilde{\epsilon}_i = \epsilon_i + \chi_i |E|^2 \approx \epsilon_i + \chi_i \langle |E|^2 \rangle_i . \tag{15}$$

For two-component nonlinear composite media, Eqs. (12) and (13) are then modified as

$$f\langle |E|^2 \rangle_1 = \int_0^1 \frac{|\tilde{s}|^2 m(x)}{|\tilde{s}-x|^2} dx E_0^2, \tag{16}$$

$$(1-f)\langle |E|^2 \rangle_2 = \left[ 1 - \int_0^1 \frac{(|\tilde{s}|^2 - x) m(x)}{|\tilde{s}-x|^2} dx \right] E_0^2, \tag{17}$$

where $\tilde{s} \equiv \tilde{\epsilon}_2/(\tilde{\epsilon}_2 - \tilde{\epsilon}_1)$. Note that $\langle |E|^2 \rangle_i$ in Eqs. (16) and (17) is the average of the local field squared inside nonlinear component $i$ $(=1,2)$. In fact, Eqs. (16) and (17) have been used to investigate the effective nonlinear response of strongly nonlinear composite media, where the linear part in Eq. (14) vanishes [19], and applied to the study of nonlinear alternating current response of colloidal suspensions [20], where the linear and nonlinear parts in Eq. (15) are comparable. In this paper, we shall adopt them to study the optical bistability of the nonlinear composite media. Fortunately, it can self-consistently be solved from a couple of equations [Eqs. (16) and (17)], as long as spectral density function $m(x)$ is given. As we know, $m(x)$ describes the geometric information of the composite under consideration. Hence, once a certain microstructure is given, its corresponding $m(x)$ can be calculated.

### B. Self-consistent mean field approximation for Maxwell-Garnett type microstructures

We shall investigate the optical bistable behavior in a nonlinear two-phase composite, in which nonlinear spheroidal metallic granular inclusions of volume fraction $f$ are randomly embedded in a nonlinear dielectric host. All the spheroidal particles have different sizes, but are assumed to exist in the form of the same shape which is characterized by depolarization factors $L_z$ along the $z$ axis and $L_{xy} \equiv (1 - L_z)/2$ along the $x$ (or $y$) axis. Since the axes of the spheroidal particles are randomly distributed in space, the effective nonlinear response will become isotropic.

This kind of microgeometric structure admits the following spectral density function in terms of a sum of two $\delta$ functions [12],

$$m(x) = F_1 \delta(x - s_1) + F_2 \delta(x - s_2), \tag{18}$$

where the poles $s_1$ and $s_2$ are given by

$$s_1 = \tfrac{1}{12}[3 - 2f + 3L_z + \sqrt{(2f - 3 - 3L_z)^2 - 72(1-f)(1-L_z)L_z}], \tag{19}$$

$$s_2 = \tfrac{1}{12}[3 - 2f + 3L_z - \sqrt{(2f - 3 - 3L_z)^2 - 72(1-f)(1-L_z)L_z}], \tag{20}$$

and the corresponding residues $F_1$ and $F_2$ have the form

$$F_1 = \frac{f}{6} \frac{1 + 3L_z - 6s_1}{s_2 - s_1} \quad \text{and} \quad F_2 = \frac{f}{6} \frac{1 + 3L_z - 6s_2}{s_1 - s_2}. \tag{21}$$

Note that the two residues satisfy the sum rule $F_1 + F_2 = f$, as expected.

The substitution of Eq. (18) into Eqs. (16) and (17) yields

$$f\langle |E|^2 \rangle_1 = \left[ \frac{|\tilde{s}|^2}{|\tilde{s}-s_1|^2} F_1 + \frac{|\tilde{s}|^2}{|\tilde{s}-s_2|^2} F_2 \right] E_0^2, \tag{22}$$

$$(1-f)\langle |E|^2 \rangle_2 = \left[ 1 - \frac{|\tilde{s}|^2 - s_1}{|\tilde{s}-s_1|^2} F_1 - \frac{|\tilde{s}|^2 - s_2}{|\tilde{s}-s_2|^2} F_2 \right] E_0^2. \tag{23}$$

Next, Eqs. (22) and (23) can readily be solved in a self-consistent manner for $\langle |E|^2 \rangle_1$ and $\langle |E|^2 \rangle_2$ as a function of $E_0^2$, and hence the desired optical bistable behavior is obtained.

## III. NUMERICAL RESULTS FOR OUTPUT INTENSITY ($\langle |E|^2 \rangle_1$) AGAINST INPUT INTENSITY ($E_0^2$)

We are in a position to perform numerical calculations in an attempt to study the features of nonlinear optical properties. The linear optical parameters are set to be $\epsilon_1 = -7.1 + 0.22i$ and $\epsilon_2 = 2.0$ [9], which leads to $s \approx 0.22 + 0.005i$. For simplicity, we shall concentrate on two typical cases: one is the composite system composed of nonlinear metallic inclusions with $\chi_1 = 10^{-8}$ esu and linear dielectric host (namely, $\chi_2 = 0$); the other is the system consisting of linear metallic inclusions (i.e., $\chi_1 = 0$) and nonlinear dielectric host with $\chi_2 = 10^{-8}$ esu. In fact, our formulas hold for a more complicated case, such as, with both components being nonlinear.

To observe the optical bistability, we should calculate $\langle |E|^2 \rangle_i$ in the presence of an external intensity $E_0^2$. However, we find that, to get the input-output curves, it is easier to obtain the values of the input intensity ($E_0^2$) as a function of output intensity ($\langle |E|^2 \rangle_i$). For example, for the composite system with a linear dielectric host (i.e., $\chi_2 = 0$), as $E_0^2$ is given, Eq. (16) [or Eq. (22)] is a nonlinear equation for $\langle |E|^2 \rangle_1$ as a function of $E_0^2$; however, as $\langle |E|^2 \rangle_1$ is given, it is quite easy to calculate $E_0^2$ directly from Eq. (16) [or Eq. (22)]. For the composite system with a linear metallic inclusion ($\chi_1 = 0$), we can take one step forward to obtain $\langle |E|^2 \rangle_2$ as a function of $E_0^2$ from Eq. (17) [or Eq. (23)]. Next, we calculate $\langle |E|^2 \rangle_1$ as a function of $E_0^2$ by using Eq. (16) [or Eq. (22)].

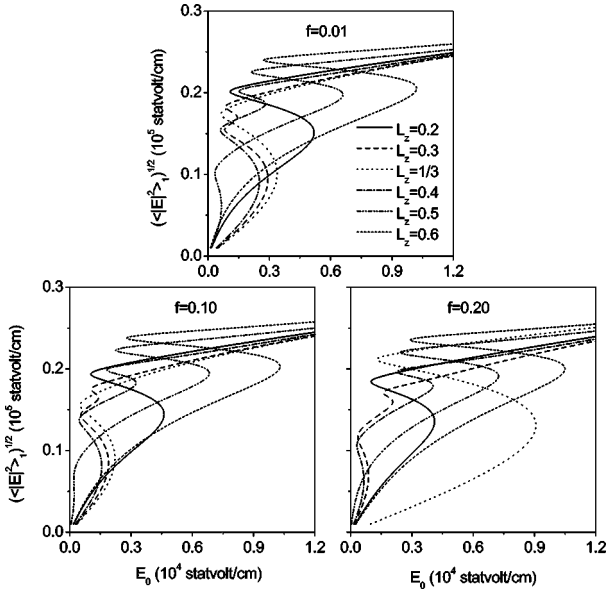


FIG. 1. $\sqrt{\langle|E|^2\rangle_1}$ vs the external field $E_0$ for $\chi_1=10^{-8}$ esu and $\chi_2=0$.

$\sqrt{\langle|E|^2\rangle_1}$ is plotted against the applied field $E_0$ for $\chi_1=10^{-8}$ esu and $\chi_2=0$ (Fig. 1), and for $\chi_1=0$ and $\chi_2=10^{-8}$ esu (Fig. 2). From the two figures, we find that the curves are strongly dependent on the depolarization factor (or particle shape) of the inclusions, whereas weakly dependent on the volume fraction. The hysteresis loops for $\langle|E|^2\rangle_i$ appear always for all $L_z$. In the dilute limit, we note that the curves for the case of $\chi_2=10^{-8}$ esu [Fig. 2(a)] are quite different from those for the case of $\chi_1=10^{-8}$ esu [Fig. 1(a)]. For instance, just after the optical hysteresis, $\sqrt{\langle|E|^2\rangle_1}$ decreases first and then increases [Fig. 2(a)], while $\sqrt{\langle|E|^2\rangle_1}$ increases monotonically for increasing $E_0$ [Fig. 1(a)]. From Figs. 1 and 2, three typical behaviors are observed; they are

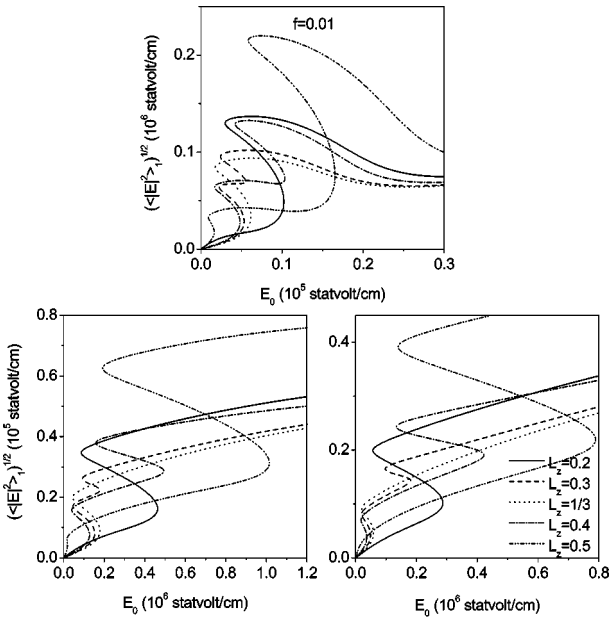


FIG. 2. Same as Fig. 1, but for $\chi_1=0$ and $\chi_2=10^{-8}$ esu.

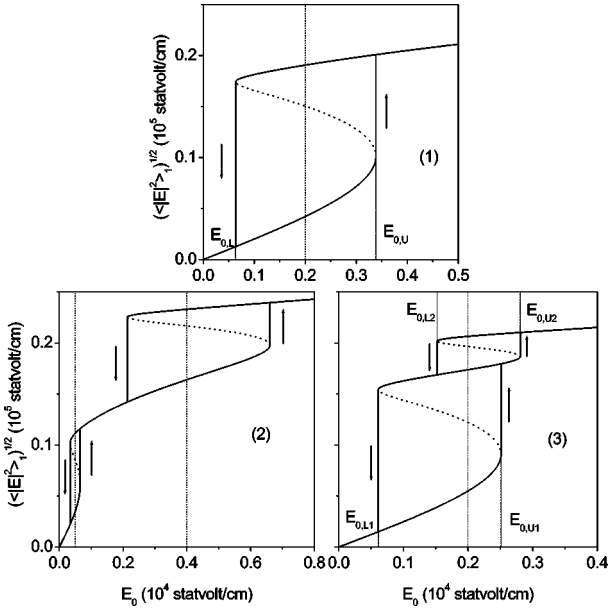


FIG. 3. Three typical behaviors in nonlinear composites for $f=0.01$ and $\chi_1=10^{-8}$ esu. They are, respectively, (1) the single bistability for $L_z=1/3$, (2) the double bistability for $L_z=0.5$, and (3) The tristability for $L_z=0.4$. The negative slop (dashed lines) represents the unsteady state. The dashed lines indicate that at the field, $\langle|E|^2\rangle_1$ may admit three or five real roots, signifying the bistable or the tristable behaviors.

(1) single optical bistability (OB), (2) double OB, and (3) optical tristability (OT), as also shown in Fig. 3. To the best of our knowledge, the behaviors of the double OB and the OT are predicted herein for the first time. For these two behaviors, when the applied field $E_0$ increases over the first upper threshold field $E_{0,U1}$, the discontinuous jump of the local field takes place from the lower branch to the middle branch; as $E_0$ further increases up to the second threshold field $E_{0,U2}$, we find the other discontinuous jump from the middle branch to the upper branch. In contrast, after $E_0$ is decreased to the lower threshold field $E_{0,L2}$, $\sqrt{\langle|E|^2\rangle_1}$ can not decrease simultaneously, but jump down to the middle branch and then follow it until $E_0$ is decreased down to the other lower threshold field $E_{0,L1}$. The difference between the double bistability and the tristability is in the following. For a given $E_0$, $\sqrt{\langle|E|^2\rangle_1}$ has three real roots within the two electric field domains, and hence the desired double bistability. However, it has five real roots in one field region, and hence the desired tristability.

In Fig. 4, we investigate the phase diagram of the single bistability, the double bistability, and the tristability in an $L_z$-$f$ plot. The phase diagram is mainly occupied by single bistability (see region 1, $L_z>0.55$, $L_z<0.22$, sor $L_z=1/3$ around). In particular, the tristability takes place in region 3, which includes two parts, one is $0.25<L_z<0.32$ for $f<0.15$ and the other is $0.35<L_z<0.42$ for $f<0.08$. For small $f$, gradually increasing $L_z$ leads to all possible transitions between the single OB, the double OB, and the OT. However, for larger volume fractions than 0.15, only one kind of phase transition appears, namely, the transition from

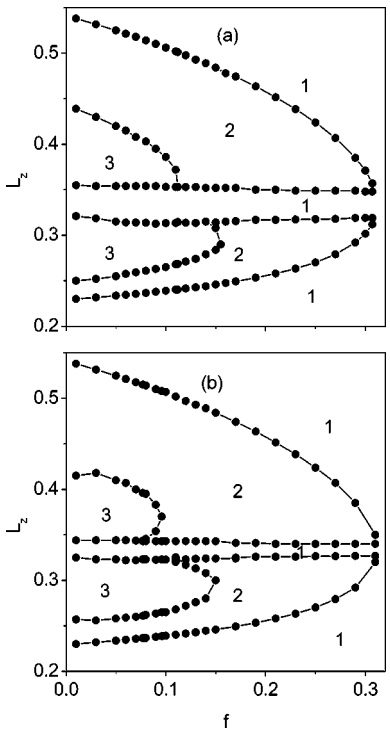


FIG. 4. Phase diagram for 1 (single bistability), 2 (double bistability), and 3 (tristability) regions is shown for (a) the nonlinear metal component with $\chi_1=10^{-8}$ esu and (b) the nonlinear dielectric component with $\chi_2=10^{-8}$ esu.

the single OB to the double OB, or from the double OB to the single OB.

To explain qualitatively the above-mentioned phenomenon in the phase diagram, we plot the poles ($s_1$ and $s_2$) and the corresponding residues ($F_1$ and $F_2$) as a function of the depolarization factor ($L_z$) (Fig. 5). For simplicity, we discuss the case where the metallic inclusions are nonlinear only.

It is found that, at a given volume fraction, the real part of $s$ [$\mathrm{Re}(s)=\mathrm{Re}\epsilon_2/(\epsilon_2-\epsilon_1)\approx 0.22$] is always smaller than $s_1$, but larger than $s_2$ for $0<L_z\leqslant 0.22$ or $L_z\geqslant 0.54$. In this region, as $\mathrm{Re}(\tilde{s})=\mathrm{Re}[\epsilon_2/(\epsilon_2-\epsilon_1-\chi_1|E|^2)]$ increases gradually with the increase of $E_0$, it becomes near to $s_1$ but far away from $s_2$. As a result, the second part of Eq. (22) is much less than the first part, and thus its contribution to $\langle|E|^2\rangle_1$ can be omitted. In this sense, Eq. (22) will becomes a cubic equation for $\langle|E|^2\rangle_1$, which signifies a single optical bistable behavior. In the region $0.24\leqslant L_z\leqslant 0.48$ (dependent on volume fractions), both poles $s_1$ and $s_2$ are larger than $\mathrm{Re}\tilde{s}$. Let us discuss the case of the poles which are well separated from each other (e.g., $f=0.2$). As $\mathrm{Re}(\tilde{s})$ becomes close to $s_2$ for increasing $E_0$, the first optical bistability appears. Furthermore, increasing $E_0$ leads to $\mathrm{Re}(\tilde{s})\approx s_1$, and thus the second optical bistability is observed. However, for $L_z\approx 1/3$ (spherical particles), we will have either $s_1\approx s_2$ for small volume fractions or $F_1\to 0$ for large volume fractions. As a result, only a single bistable behavior exists. To our interest, once the poles ($s_1$ and $s_2$) are neither too close nor too far, both contributions from $s_1$ and $s_2$ become comparable. In this situation, Eq. (22) is a fifth-order polynomial

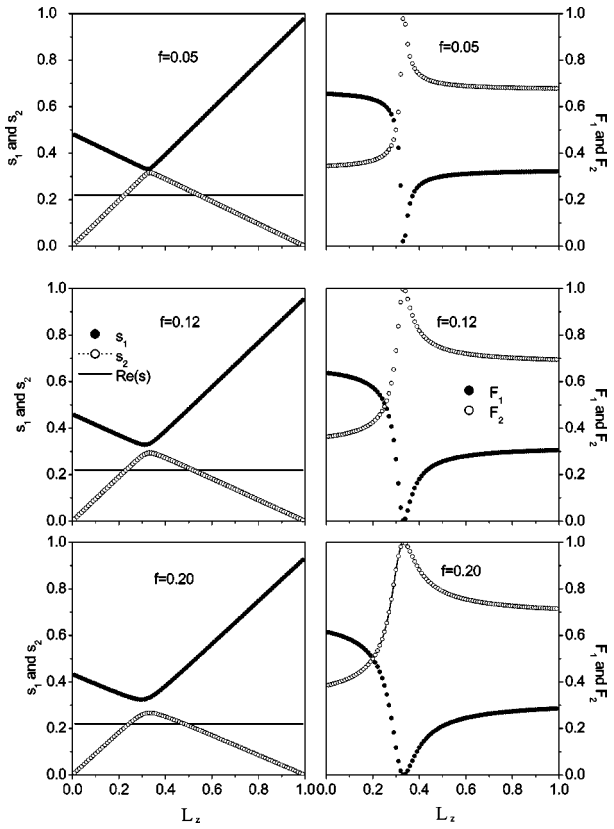


FIG. 5. Poles $s_1, s_2$ and corresponding residues $F_1, F_2$ vs $L_z$ for various $f=0.05$, 0.12, and 0.20.

equation for $\langle|E|^2\rangle_1$, which produces five real roots for a given applied field $E_0$, thus signifying the tristability.

In Fig. 6, we plot the maximum threshold field $E_{0,M}$ ($E_{0,M}=E_{0,U}$ for the single OB, and $=E_{0,U2}$ for the double OB and the OT) against $L_z$ for $f=0.05$. It is shown that $E_{0,M}$ for the nonlinear dielectric host is much larger than the one for the nonlinear metallic inclusions. This phenomenon is clearly observed, especially for $L_z>0.5$. Consequently, we conclude that, nonlinear metallic inclusions are more favorable to reduce the threshold field than nonlinear dielectric hosts, as in accord with previous observations [9].

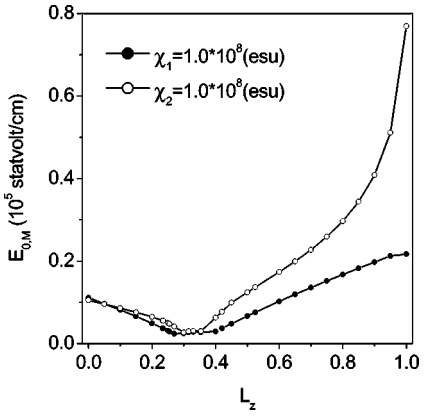


FIG. 6. Maximal threshold field $E_{0,M}$ vs $L_z$ for $f=0.05$, $\chi_1=0$, and $\chi_2=10^{-8}$ esu.

## IV. NUMERICAL RESULTS FOR NONLINEAR OPTICAL PROPERTIES

Based on our method, it is straightforward to calculate the effective dielectric constant of nonlinear composite media as a function of the external applied field $E_0$. To do so, let's consider Maxwell-Garnett type microstructures. Substituting Eq. (18) into Eq. (9), we obtain the effective linear dielectric constant ($\epsilon_e$) within the spectral representation [12]:

$$\epsilon_e = \epsilon_2\left[1 - \frac{F_1}{s - s_1} - \frac{F_2}{s - s_2}\right]. \tag{24}$$

For the nonlinear composite medium, it is supposed that the effective dielectric constant $\tilde{\epsilon}_e$ has the same form as $\epsilon_e$, i.e.,

$$\tilde{\epsilon}_e = \tilde{\epsilon}_2\left[1 - \frac{F_1}{\tilde{s} - s_1} - \frac{F_2}{\tilde{s} - s_2}\right]. \tag{25}$$

Since both $\tilde{\epsilon}_2$, $\tilde{\epsilon}_1$ (included in $\tilde{s}$) is field dependent, $\tilde{\epsilon}_e$ can be changed by adjusting applied field $E_0$. Moreover, it has been shown that the variation of $\tilde{\epsilon}_e$ becomes most strong in the vicinity of the resonant region, where $\mathrm{Re}(\tilde{s}) = s_1$ (or $s_2$) is accompanied with small $\mathrm{Im}(\tilde{s})$ [21].

Both the effective complex refractive index of nonlinear composites $\tilde{n} \equiv n + ik$ (where $n$ and $k$ are, respectively, the refractive index and the extinction coefficient) and the reflectance at normal incidence can be calculated from the following equations:

$$n = \left(\frac{\mathrm{Re}(\tilde{\epsilon}_e) + \sqrt{[\mathrm{Re}(\tilde{\epsilon}_e)]^2 + [\mathrm{Im}(\tilde{\epsilon}_e)]^2}}{2}\right)^{1/2}, \tag{26}$$

$$k = \left(\frac{-\mathrm{Re}(\tilde{\epsilon}_e) + \sqrt{[\mathrm{Re}(\tilde{\epsilon}_e)]^2 + [\mathrm{Im}(\tilde{\epsilon}_e)]^2}}{2}\right)^{1/2}, \tag{27}$$

$$R = \left|\frac{\sqrt{\tilde{\epsilon}_e} - 1}{\sqrt{\tilde{\epsilon}_e} + 1}\right|^2. \tag{28}$$

In Figs. 7–9, $n$, $k$, and $R$ are plotted as a function of $E_0$, respectively. For the sake of simplicity, we show the numerical results for nonlinear composite media where $\chi_1 = 0$ and $\chi_2 = 10^{-8}$ esu only (in fact, for the other case where $\chi_1 = 10^{-8}$ esu and $\chi_2 = 0$, similar behavior can be found). It is evident that hysteresis loops (shown in Fig. 10) for these nonlinear optical properties occur, which implies that multiple states do exist for the nonlinear composite media, corresponding to different local field distributions (Fig. 2). As a matter of fact, these different states indicate quite different physical properties that the composites possess. For example, as far as $R$ is concerned, at $E_0 = 3000$ statvolt/cm, $L_z = 0.4$ and $f = 0.2$, $\max(R)/\min(R) \approx 9$. In view of possible technological applications, this finding is expected to be very useful. Also, we note that $R$ exhibits similar behavior as $n$ ($k$) for small (large) $f$. From these figures, we conclude that oblate spheroidal metallic inclusions with small volume fractions are able to play an important role in getting a broader bistability domain.

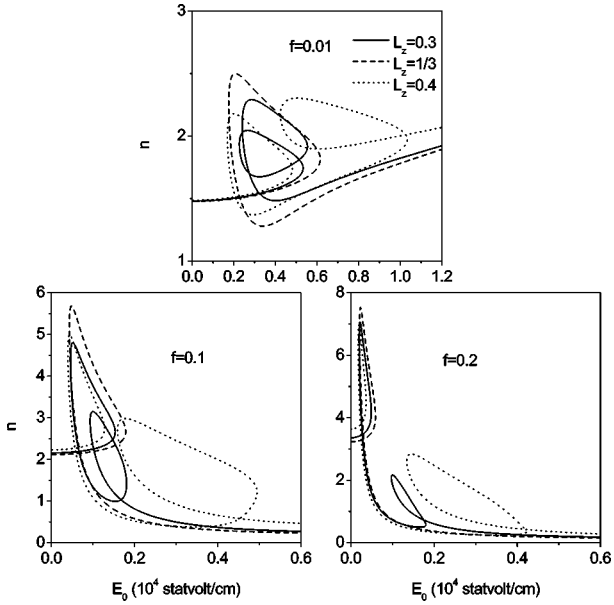


FIG. 7. The refractive index $n$ vs $E_0$ for $\chi_1 = 0$ and $\chi_2 = 10^{-8}$ esu.

## V. DILUTE LIMIT CASE AND COMPARISON WITH THE VARIATIONAL APPROACH

In what follows, we shall discuss a certain composite which contains nonlinear randomly-oriented spheroids embedded in a linear dielectric host, so that we could demonstrate the validity of our method. The composite under consideration is in the dilute limit, and subject to an external applied field $E_0$ along the direction of the $z$ axis. It is known that the local field inside the spheroids is uniform, even for nonlinear inclusions [22].

Without loss of generality, we take the principal axis of the spheroid to be oriented at angle $\theta$ to the $z$ axis. In this case, the local field $E_1$ inside the nonlinear spheroid is uni-

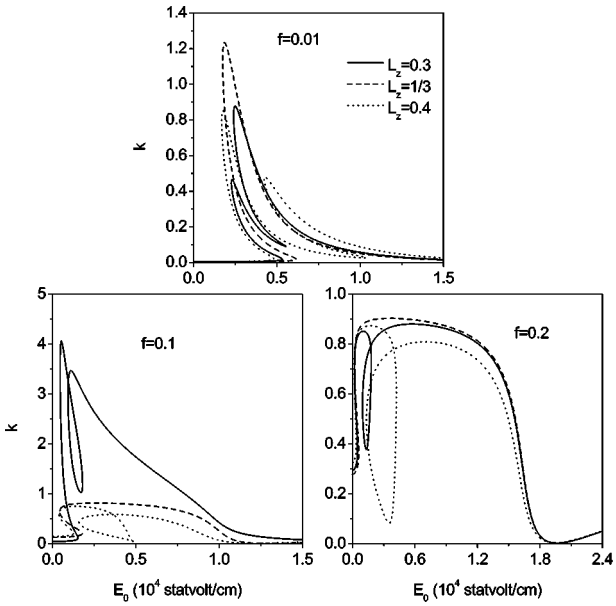


FIG. 8. Similar to Fig. 6, but for extinction coefficient $k$ vs $E_0$.

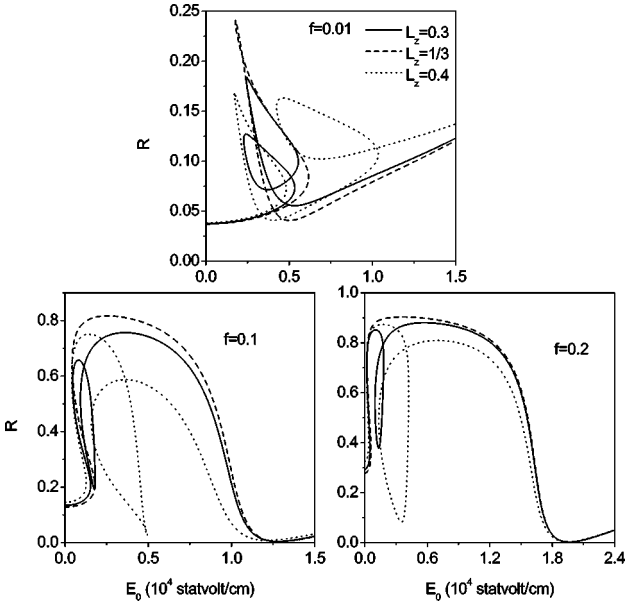


FIG. 9. Similar to Fig. 6, but for the reflectance at normal incidence $R$ vs $E_0$.

form as well, and has the form

$$\mathbf{E}_1=\frac{\epsilon_2}{\epsilon_2+L_z(\tilde{\epsilon}_1-\epsilon_2)}E_0\cos\theta\mathbf{e}_z + \frac{\epsilon_2}{\epsilon_2+L_{xy}(\tilde{\epsilon}_1-\epsilon_2)}E_0\sin\theta\cos\phi\mathbf{e}_x + \frac{\epsilon_2}{\epsilon_2+L_{xy}(\tilde{\epsilon}_1-\epsilon_2)}E_0\sin\theta\sin\phi\mathbf{e}_y, \tag{29}$$

with $\tilde{\epsilon}_1\equiv\epsilon_1+\chi_1|E|^2$.

Then, the local field squared $|E|_1^2\equiv\mathbf{E}_1^*\cdot\mathbf{E}_1$ is given by

$$|E|_1^2=\left[\left|\frac{\epsilon_2}{\epsilon_2+L_z(\tilde{\epsilon}_1-\epsilon_2)}\right|^2\cos^2\theta + \left|\frac{\epsilon_2}{\epsilon_2+L_{xy}(\tilde{\epsilon}_1-\epsilon_2)}\right|^2\sin^2\theta\right]E_0^2. \tag{30}$$

In the light of the rule

$$\langle f(\theta,\phi)\rangle=\frac{1}{4\pi}\int_0^{2\pi}\int_0^{2\pi}f(\theta,\phi)\sin\theta d\theta d\phi, \tag{31}$$

the spatial average of the local field squared within the spheroidal particles is determined by

$$\langle|E|^2\rangle_1=\left[\frac{1}{3}\left|\frac{\epsilon_2}{\epsilon_2+L_z(\tilde{\epsilon}_1-\epsilon_2)}\right|^2+\frac{2}{3}\left|\frac{\epsilon_2}{\epsilon_2+L_{xy}(\tilde{\epsilon}_1-\epsilon_2)}\right|^2\right]E_0^2. \tag{32}$$

Note Eq. (32) is exact, and it can be applied to investigate the optical bistability for a dilute suspension of randomly oriented spheroidal particles in a linear host.

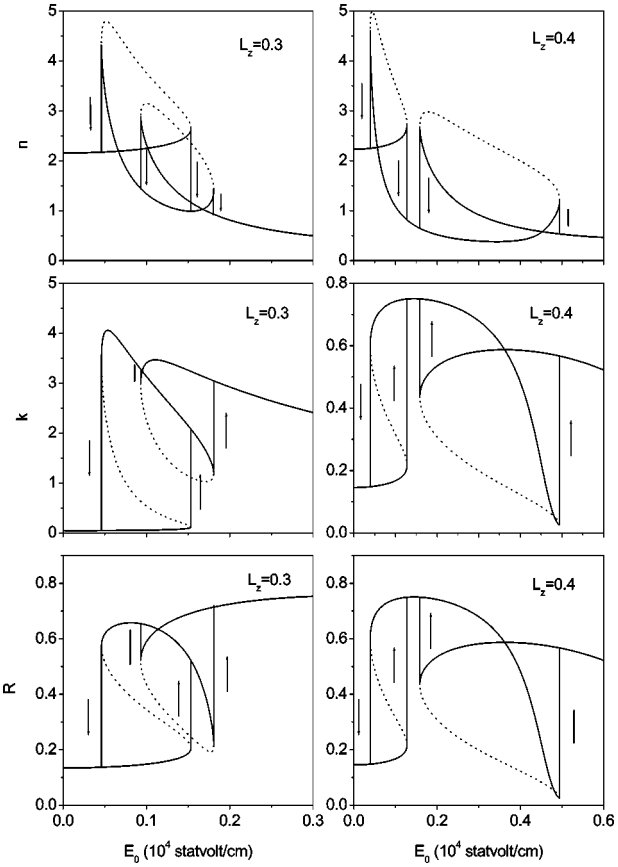


FIG. 10. Typical hysteresis loops for $n$, $k$, and $R$ at $f=0.1$, $\chi_1=0$, and $\chi_2=10^{-8}$ esu.

By using our method, in the dilute limit (namely, $f\to0$), Eqs. (19) and (20) reduce to

$$s_1=L_z \quad \text{and} \quad s_2=L_{xy}. \tag{33}$$

In this case, the residues $F_1$ and $F_2$ [Eq. (21)] become

$$F_1=\frac{f}{3} \quad \text{and} \quad F_2=\frac{2f}{3}. \tag{34}$$

Then, the substitution of Eqs. (33) and (34) into Eq. (22) yields the same formula as Eq. (32).

Now, we are in a position to study the optical bistability of the composite media composed of *linear* spherical inclusions, which are embedded in a *nonlinear* dielectric host. To compare our method with the variational approach, we set the relevant parameters to be the same as those used in Ref. [5]. To this end, our method predicts the onset of the bistable behavior with $E_{0,\text{onset}}\approx726$ statvolt/cm (onset applied field) at $f\approx0.0035$. This onset field is related to the threshold intensity $I\approx1.23\times10^8$ W/cm$^2$, which is of about two orders larger than $I=1.4\times10^6$ W/cm$^2$ predicted by the variational approach. This discrepancy should result from the fact that the present method determines self-consistently $\langle|E|^2\rangle$,

rather than $\langle|E|\rangle$, while the latter ($\langle|E|\rangle$) is determined by the variational approach [5], without the use of self-consistency.

## VI. DISCUSSION AND CONCLUSION

In this work, we have developed a general method in an attempt to study the optical bistability in two-phase nonlinear composite materials. This method allows us to solve self-consistently the relation between the average of the local field squared $\langle|E|^2\rangle_i$ within nonlinear component $i$ and the external field squared $E_0^2$, without regarding the nonlinear properties as a small perturbation to the linear behavior. In this connection, it is worth mentioning an alternative work [17], in which the authors considered the intrinsic optical bistability by using the spectral form between $\langle E\rangle_1$ and $E_0$. To determine $\langle E\rangle_1$, the rough approximation $\langle|E|^2\rangle_1 \approx |E_1|^2$ was adopted. Furthermore, the formula in Ref. [17] was only valid to the composites with a single nonlinear component.

In particular, our general framework has been illustrated in composite media consisting of nonlinear metallic inclusions randomly oriented and embedded in a nonlinear dielectric host. We find that the optical bistable behavior is dependent both on the volume fraction and the inclusion shape. Above all, new phenomena such as the double bistability and the tristability are reported in the above-mentioned nonlinear composites. In the tristability region, the composites can exhibit three different physical states for a given $E_0$, and thus this raises the interesting question of how one state is to be selected over another, and how one can switch the system between these different states [23].

In addition, since the materials have the advantage of a low absorption coefficient [24], the metallic particles may be packed up to a large volume fraction. In this case, dipole-dipole interactions should be taken into account. In this regard, the Shalaev-Sarychev theory [25] is expected to help. Work is in progress along this direction, and will be reported elsewhere.

To sum up, we have generalized our recently derived Maxwell-Garnett approximation to investigate the optical bistability of nonlinear spherical inclusions in a nonlinear dielectric host [12,26]. To our great interest, double bistability, or tristability, can be observed by adjusting the appropriate parameters.

## ACKNOWLEDGMENTS

This work was supported by the National Natural Science Foundation of China for financial support under Grant No. 10204017 and by the Natural Science of Jiangsu Province for financial support under Grant No. BK2002038. L.G. thanks Professor K. W. Yu for the useful discussions and Dr. J. P. Huang for the assistance in preparing the final version of this paper.

[1] K.M. Leung, Phys. Rev. A **33**, 2461 (1986).
[2] J.W. Haus, N. Kalyaniwalla, R. Inguva, M. Bloemer, and C.M. Bowden, J. Opt. Soc. Am. B **6**, 797 (1989).
[3] J.W. Haus, R. Inguva, and C.M. Bowden, Phys. Rev. A **40**, 5729 (1989).
[4] N. Kalyaniwalla, J.W. Haus, R. Inguva, and M.H. Birnboim, Phys. Rev. A **42**, 5613 (1990).
[5] D.J. Bergman, O. Levy, and D. Stroud, Phys. Rev. B **49**, 129 (1994).
[6] R. Levy-Nathansohn and D.J. Bergman, J. Appl. Phys. **77**, 4263 (1995).
[7] R. Neuendorf, M. Quinten, and U. Kreibig, J. Appl. Phys. **104**, 6348 (1996).
[8] K.P. Yuen and K.W. Yu, J. Phys.: Condens. Matter **9**, 4669 (1997).
[9] T. Pan and Z.Y. Li, Phys. Status Solidi B **218**, 591 (2000).
[10] A. Pinchuk, J. Phys. D **36**, 460 (2003).
[11] Y.M. Wu, L. Gao, and Z.Y. Li, Phys. Status Solidi B **220**, 997 (2000).
[12] L. Gao, Jones T.K. Wan, K.W. Yu, and Z.Y. Li, J. Phys.: Condens. Matter **12**, 6825 (2000).
[13] K.W. Yu, P.M. Hui, and H.C. Lee, Phys. Lett. A **210**, 115 (1996).
[14] W.M.V. Wan, H.C. Lee, P.M. Hui, and K.W. Yu, Phys. Rev. B **54**, 3946 (1996).
[15] L. Gao and Z.Y. Li, Phys. Lett. A **219**, 324 (1996).
[16] D.J. Bergman, Phys. Rep. **43**, 377 (1978).
[17] O. Levy and D.J. Bergman, Physica A **207**, 157 (1994).
[18] H.R. Ma, R.F. Xiao, and P. Sheng, J. Opt. Soc. Am. B **15**, 1022 (1998).
[19] K.W. Yu, Solid State Commun. **105**, 689 (1998).
[20] J.P. Huang, L. Gao, and K.W. Yu, J. Appl. Phys. **93**, 2871 (2003).
[21] O. Levy, Y. Yagil, and D.J. Bergman, J. Appl. Phys. **76**, 1431 (1994).
[22] L.D. Landau, E.M. Lifshitz, and L.P. Pitaevskii, *Electrodynamics of Continuous Media*, 2nd ed. (Pergamon, New York, 1984), Chap. 2.
[23] L. Fu and L. Resca, Solid State Commun. **105**, 413 (1998).
[24] A.E. Neeves and M.H. Birnboim, J. Opt. Soc. Am. B **6**, 787 (1989); Opt. Lett. **13**, 1087 (1988).
[25] A.K. Sarychev and V.M. Shalaev, Phys. Rep. **335**, 275 (2000), and references cited therein.
[26] L. Gao, K.W. Yu, Z.Y. Li, and Bambi Hu, Phys. Rev. E **64**, 036615 (2001).